Original article
UDC 620.92; 539.232; 538.9; 535.215.6
DOI: https://doi.org/10.18721/JPM.19103

TEMPERATURE EFFECTS ON THE LIGHT CURRENT-VOLTAGE CHARACTERISTICS OF THE HETEROJUNCTION SOLAR CELLS FABRICATED ON GALLIUM-DOPED SILICON SUBSTRATES

O. K. Ataboev [1] ✉, Sh. B. Utamuradova [1], E. I. Terukov [2], A. I. Baranov [3], K. Kh. Iniyatova [4]

[1] Research Institute of Semiconductor Physics and Microelectronics at the National University of Uzbekistan named after Mirzo Ulugbek, Tashkent, Republic of Uzbekistan;
[2] Ioffe Institute, RAS, St. Petersburg, Russia;
[3] Alferov University, RAS, St. Petersburg, Russia;
[4] Nukus State Technical University, Nukus, Karakalpakstan, Republic of Uzbekistan

✉ omonboy12@mail.ru

Abstract. In this study, the impacts of temperature on the light current-voltage characteristics of heterojunction solar cells fabricated on gallium-doped crystalline *p*-type silicon (c-Si) has been studied under air mass zero spectrum (136.7 mW/cm²) in the temperature range from 173 to 373 K. Our experimental results indicated that the short-circuit current density increased linearly with temperature, exhibiting a positive temperature coefficient of 0.058%/K, whereas the open-circuit voltage (V_{oc}) decreased linearly. From the experiment, the calculated temperature coefficient value of the V_{oc} was found to be –0.182%/K. Both the maximum output power and conversion efficiency of the heterojunction solar cells increased linearly with decreasing temperature from 373 K, reaching peak values of ~29.5 mW/cm² and ~21.5% at 173 K. The temperature coefficient of the maximum output power was evaluated to be –0.2%/K, which represents one of the record-breaking small values reported among SCs based on other single c-Si technologies.

Keywords: heterojunction solar cell, temperature dependence, open-circuit voltage, conversion efficiency, temperature coefficient

Funding: The reported study was funded by Russian Science Foundation (Grant No. 24-79-10275).

For citation: Ataboev O. K., Utamuradova Sh. B., Terukov E. I., Baranov A. I., Iniyatova K. Kh., Temperature effects on the light current-voltage characteristics of the heterojunction solar cells fabricated on gallium-doped silicon substrates, St. Petersburg State Polytechnical University Journal. Physics and Mathematics. 19 (1) (2026) 30–42. DOI: https://doi.org/10.18721/JPM.19103

This is an open access article under the CC BY-NC 4.0 license (https://creativecommons.org/licenses/by-nc/4.0/)

© Ataboev O. K., Utamuradova Sh. B., Terukov E. I., Baranov A. I., Iniyatova K. Kh., 2026. Published by Peter the Great St. Petersburg Polytechnic University.

Научная статья
УДК 620.92; 539.232; 538.9; 535.215.6
DOI: https://doi.org/10.18721/JPM.19103

ВЛИЯНИЕ ТЕМПЕРАТУРЫ НА СВЕТОВЫЕ ВОЛЬТАМПЕРНЫЕ ХАРАКТЕРИСТИКИ ГЕТЕРОСТРУКТУРНЫХ СОЛНЕЧНЫХ ЭЛЕМЕНТОВ, ИЗГОТОВЛЕННЫХ НА ПОДЛОЖКАХ КРЕМНИЯ, ЛЕГИРОВАННОГО ГАЛЛИЕМ

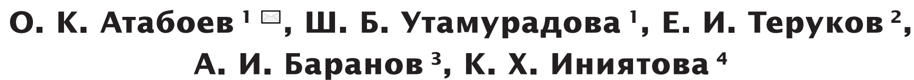

О. К. Атабоев [1] ✉, Ш. Б. Утамурадова [1], Е. И. Теруков [2], А. И. Баранов [3], К. Х. Иниятова [4]

[1] Научно-исследовательский институт физики полупроводников и микроэлектроники при Национальном университете Узбекистана имени М. Улугбека, г. Ташкент, Республика Узбекистан;

[2] Физико-технический институт имени А. Ф. Иоффе РАН, Санкт-Петербург, Россия;

[3] Академический университет имени Ж. И. Алфёрова РАН, Санкт-Петербург, Россия;

[4] Нукусский государственный технический университет, г. Нукус, Каракалпакстан, Республика Узбекистан

✉ omonboy12@mail.ru

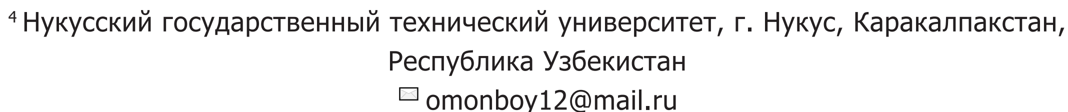

Аннотация. В работе исследовано влияние температуры на световые вольтамперные характеристики гетероструктурных солнечных элементов (изготовлены на кремнии *p*-типа, легированном галлием) при нулевой воздушной массе (поверхностная плотность потока энергии 136,7 мВт/см^2) в температурном диапазоне 173 – 373 K. Экспериментальные результаты показали, что плотность тока короткого замыкания линейно возрастает с повышением температуры, демонстрируя положительный температурный коэффициент 0,058%/K, тогда как напряжение холостого хода V_{oc} линейно снижается. Температурный коэффициент V_{oc}, рассчитанный по результатам эксперимента, составил –0,182%/K. Максимальная выходная мощность и коэффициент преобразования гетероструктурных солнечных элементов линейно увеличивались при понижении температуры от 373 K, достигая максимальных значений (около 29,5 мВт/см^2 и 21,5% при 173 K). Согласно оценке, температурный коэффициент максимальной выходной мощности составил всего –0,2%/K, что является одним из рекордно малых значений для солнечных элементов на основе других технологий монокристаллического кремния.

Ключевые слова: гетеропереходный солнечный элемент, температурная зависимость, напряжение холостого хода, эффективность преобразования, температурный коэффициент

Финансирование: Исследование выполнено при финансовой поддержке Российского научного фонда (грант № 24-79-10275).

Для цитирования: Атабоев О. К., Утамурадова Ш. Б., Теруков Е. И., Баранов А. И., Иниятова К. Х. Влияние температуры на световые вольтамперные характеристики гетероструктурных солнечных элементов, изготовленных на подложках кремния, легированного галлием // Научно-технические ведомости СПбГПУ. Физико-математические науки. 2026. Т. 19. № 1. С. 30–42. DOI: https://doi.org/10.18721/ JPM.19103

Статья открытого доступа, распространяемая по лицензии CC BY-NC 4.0 (https://creativecommons.org/licenses/by-nc/4.0/)

© Атабоев О. К., Утамурадова Ш. Б., Теруков Е. И., Баранов А. И., Иниятова К. Х., 2025. Издатель: Санкт-Петербургский политехнический университет Петра Великого.

Introduction

In recent years, the global demand for renewable energy sources has shown a consistent upward trend. This increase is largely driven by the progressive depletion of fossil fuel resources, rapid economic growth, and the ongoing expansion of industrial sectors. Consequently, to mitigate the emerging energy shortfall, a worldwide shift toward renewable energy technologies – particularly solar PhotoVoltaic (PV) one is becoming increasingly prominent [1]. Among the various renewable energy technologies, PV systems based on silicon (Si), cadmium telluride (CdTe), copper-indium-gallium-selenide ($CuIn_xGa_{1-x}Se_2$), copper-zinc-tin-selenide (CuZnSnSe) (the last two are abbreviated as CIGS and CZTS), and perovskite materials represent the most prominent and rapidly advancing solutions due to their scalability, efficiency, and compatibility with diverse applications [2].

Currently, silicon-based solar cells (SCs) dominate the global PV market, accounting for over 95% of the total market share. This dominance is largely attributed to the maturity of Si fabrication technologies and the widespread availability of Si as a raw material [3]. Among Si-based PV technologies, silicon heterojunction solar cells (HJT SCs) have attracted considerable attention owing to their high-efficiency architecture. As a result, HJT SCs have achieved high conversion efficiencies of up to 27.1% for *n*-type and 26.6% for *p*-type Si substrates, significantly surpassing the performance of passivated emitter and rear contact (abbreviated as PERC) and conventional homojunction cells [4, 5]. Moreover, this type SCs have a higher bifacial coefficient compared to other Si-based technology SCs [6]. These advantages make HJT SCs highly attractive not only for terrestrial applications but also for space applications.

To date, the performance of SCs has been mainly evaluated under the standard test conditions (AM1.5G, 100 mW/cm^2) in the temperature range from 10 to 80°C. However, there is a notable lack of data regarding the PV behavior of SCs at sub-zero temperatures, particularly under air mass zero (AM0) irradiation conditions, which are representative of space environments [7, 8]. According to Refs. [9, 10], spacecrafts in low-Earth orbit (LEO) travel at approximately 8 km/s and complete one orbit around the Earth every 90 minutes. As the spacecraft passes through each orbit, it either enters the illuminated (sunlit) side of the Earth or shadowed (dark) one. As a result, the temperature on the sunlit side can rise up to 100°C (373 K), while on the dark side and during transitions into and out of the Earth's shadow, the temperature can drop as low as −100°C (173 K).

Based on the above-mentioned, here we explore the influence of temperature on the light *J-V* curves of HJT SCs fabricated on gallium-doped *p*-type c-Si substrates. The light *J-V* curves were systematically analyzed over a broad temperature range from 173 to 373 K under AM0 (air mass zero) spectral conditions (flux surface density of the electromagnetic energy was 136.7 mW/cm^2).

Material preparation and methods

Sample preparation. The investigated HJT SCs were fabricated at R&D Center of Thin film technologies in Energetics, Saint-Petersburg, Russian Federation. To perform investigation, Si HJT SCs (Fig. 1) were created on gallium-doped *p*-type c-Si substrates grown by the Czochralski (Cz) method, with an acceptor concentration of $N_a \geq 3.1 \cdot 10^{16}$ cm^{-3}, a thickness of ~135 μm, crystallographic orientation (100) and with an initial bulk minority carrier lifetime of $\tau_{bulk} \geq 0.2$ ms. In the c-Si substrate, the oxygen concentration was ~$2.5 \cdot 10^{17}$ cm^{-3}, the carbon concentration was ~$2 \cdot 10^{16}$ cm^3, and the dislocation density was ~500 cm^{-3}.

Initially, *p*-type c-Si substrates underwent a wet chemical cleaning procedure. After that, substrates were subjected to pyramidal surface texturing in order to minimize incident light reflection and enhance the short-circuit current density (J_{sc}) of the HJT SCs [11]. Next, thin intrinsic hydrogenated amorphous silicon (*i*-α-Si:H) layers ~5 nm thick were deposited on both front and rear surfaces of the textured substrates using Radio-Frequency Plasma-Enhanced Chemical Vapor Deposition method (RF PECVD). The purpose of this layer was to passivate dangling bonds (Si – H) on the surfaces of Si substrates [12]. Using the same method to form *p–n* junction, heavy doped n^+-type α-Si:H layers were deposited on the front side of the *i*-α-Si:H coated *p*-type c-Si substrates. Simultaneously, to create the back-surface field (BSF), heavy doped p^+-type α-Si:H layers were deposited on the rear sides of *i*-α-Si:H deposited *p*-type c-Si substrates. The thicknesses of both the front and rear n^+-type and p^+-type α-Si:H layers were kept identical (they were from 10 to 15 nm). To obtain p^+-type and n^+-type conductivity in

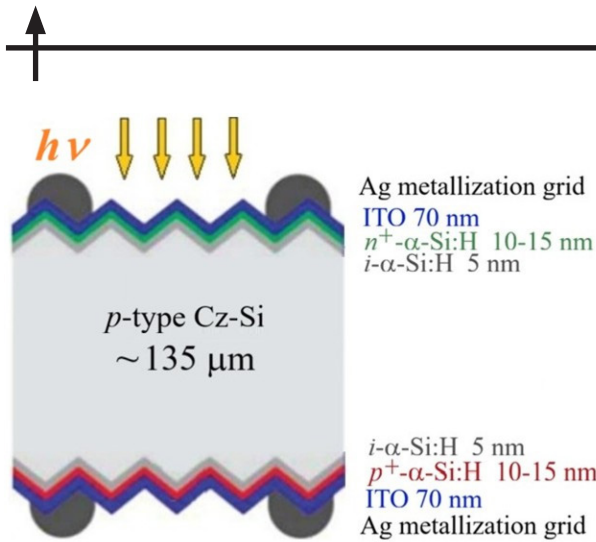

Fig. 1. A cross-section view of the finished HJT SCs based on *p*-type c-Si substrates

the α-Si:H layers respectively, the monosilane (SiH_4) gas was diluted with (high-purity, 99.999%) diborane (B_2H_6) and phosphine (PH_3) gases. All α-Si:H layers were deposited at a low temperature from 180 to 185°C with a frequency of 40.68 MHz. Further, transparent conductive oxide (TCO) layers composed of indium tin oxide (ITO – 90 wt.% In_2O_3 and 10 wt.% SnO_2), a thickness of ~70 nm, were deposited on the front and rear surfaces of the photosensitive heterostructures using Radio-Frequency (RF) magnetron sputtering. To collect photogenerated charge carriers from the heterostructure surfaces, silver (Ag) paste was screen-printed onto both the front and rear sides of the photosensitive heterostructures. The "Busbar" type contacts had a height of ~25 μm, a width of ~45 μm, and were patterned with a pitch of ~1.36 mm. A view of the HJT SCs is shown in Fig. 1.

To perform experiment, samples measuring 1 × 1 cm were cut from a high-efficiency HJT SCs with the full size 15.6 × 15.6 cm. After cutting, no additional passivation was applied to the lateral surfaces, and the edge isolation was not done. A solid-state "MiniMaker2" diode laser with a wavelength of 1064 nm was used to cut the samples.

This study has focused on characterizing the temperature-dependent performance of *p*-type c-Si HJT SCs in the temperature range from 173 to 373 K, without considering radiation effects.

Characterization and measurement of performances. To study the effect of temperature on the light *J-V* curves of HJT SCs, these curves were measured using a liquid nitrogen cryostat (Janis VPF-100) in the temperature range from 173 to 373 K, in 20 K increments. In the course of the measurements, the samples were illuminated by a class AAA pulsed solar simulator (SS-80AA simulator) under AM0 spectral conditions (136.7 mW/cm^2). The short-circuit current density (J_{SC}) and open-circuit voltage (V_{oc}) were recorded using a Keithley SM2460 Source Meter.

In the course of the measurements, temperature stabilization was achieved using a liquid nitrogen cryostat equipped with temperature monitoring device, namely, a Lake Shore Model 335 temperature controller having a control accuracy of ±0.1°C. Each measurement of the light *J-V* curves was conducted after the target temperature was reached and maintained for 4 – 5 min under AM0 spectrum (136.7 mW/cm^2). Temperature coefficients of the output parameters of the HJT SCs, such as the open-circuit voltage (V_{oc}), the short-circuit current density (J_{sc}), the fill factor (*FF*), the maximum output power (P_{max}) and the conversion efficiency (η) were extracted from the slopes of the straight-line portions of the experimental temperature-dependent curves.

About 30 HJT SCs samples were fabricated for the investigation. They had similar parameters within a margin of error of no more than 2%. Of these samples, only one, measuring 1 × 1 cm, was selected for the temperature-dependence investigation.

Results and discussion

Theoretical formulation of the open-circuit voltage versus temperature. It has been reliably established that the key PV parameters of HJT SCs, such as V_{oc}, J_{sc}, *FF*, P_{max} and η exhibit significant temperature dependence. Among them, V_{oc} is the most sensitive to ambient temperature, demonstrating a pronounced decrease as the temperature goes up, which in turn leads to a significant reduction in the η value of the HJT SCs [13, 14].

To interpret the experimental temperature dependence $V_{oc}(T)$ for the HJT SCs (see further Fig. 3, *b*), we employed a current transport model previously reported in [15, 16]. This model enables the analysis of solar cell performance under arbitrary injection conditions and for any ratio of carrier diffusion length (L_{diff}) to substrate thickness (*d*). To derive the fundamental equations, an n^+–p–p^+ heterostructure was considered, accounting for the electronic properties of both the n^+–p and p–p^+ heterojunctions. By applying appropriate boundary conditions at the interfaces, the key expression describing the of $V_{oc}(T)$ was obtained. A comprehensive derivation and discussion

of these equations are provided in our previous work [17]. Therefore, only a brief overview is presented in this study.

It is well known that when a solar cell is illuminated with white light, nonequilibrium electron-hole pairs are photogenerated within the base region. These carriers are separated by the built-in electric field at the heterojunction, resulting in the generation of photocurrent. Consequently, the equivalent electrical circuit of a HJT SCs can be modeled through an ideal current source of density J_{sc}. Under this illumination condition, the corresponding boundary conditions are defined as follows:

$$\frac{d\Delta n}{dx} = -\frac{J - J_{surf}}{qD} \text{ at } x = 0, \ \frac{d\Delta n}{dx} = 0 \text{ at } x = d, \tag{1}$$

where q is the elementary charge, J_{surf} is the total surface recombination current density, d is the c-Si substrate thickness, Δn is the excess carrier concentration;

$$J_{surf} = qS_0 \Delta n_{(x=0)} + qS_d \Delta n_{(x=d)},$$

where S_0, S_d are the surface recombination velocities on the front and rear surfaces of substrate, respectively.

Taking into consideration the theoretical framework established in our previous work [16], as well as the boundary conditions (1), the following analytical expression for the current density J was derived:

$$J = \frac{\sinh\left(\frac{d}{L_{diff}}\right)}{\cosh\left(\frac{d-x}{L_{diff}}\right)} \left(-qGL_{diff} + \frac{qD\Delta n(x)}{L_{diff}}\right) + J_{surf}, \tag{2}$$

at the boundary of the n^+–p heterojunction (for the cross-section $x = 0$) Eq. (2) takes the form:

$$J = -J_{sc} + \frac{qD\Delta n_{(x=0)}}{L_{diff}} \cdot \tanh\left(\frac{d}{L_{diff}}\right) + J_{surf}, \tag{3}$$

where

$$J_{sc} = qGL_{diff} \tanh\left(\frac{d}{L_{diff}}\right). \tag{4}$$

The voltage V drops across the HJT SC structure is predominantly determined by the forward bias applied to the n^+–p heterojunction [15, 16]:

$$V = \frac{kT}{q} \ln\left[\frac{\Delta n\left(\Delta n + N_a\right)}{n_i^2\left(T\right)}\right], \tag{5}$$

where $n_i(T)$ is the intrinsic equilibrium carrier concentration in the substrate at a given temperature T; k is the Boltzmann constant.

Under open-circuit conditions ($J = 0$), the excess carrier concentration Δn is uniform over all cross-sections of the substrate and,

$$\Delta n(V_{oc}) = \frac{J_{sc}}{q\left[\frac{D}{L_{diff}} \tanh\left(\frac{d}{L_{diff}}\right) + S\right]}, \tag{6}$$

where $S = S_0 + S_d$.

Open circuit voltage V_{oc} can be estimated as

$$V_{oc}(T) = \frac{E_g(T)}{q} - \frac{kT}{q}\ln\left\{\frac{N_{co}N_{Vo}}{\left[\dfrac{J_{sc}(T)}{q\left[\dfrac{D}{L_{diff}}\tanh\left(\dfrac{d}{L_{diff}}\right)+S(T)\right]}\right]\left[N_a(T)+\dfrac{J_{sc}(T)}{q\left[\dfrac{D}{L_{diff}}\tanh\left(\dfrac{d}{L_{diff}}\right)+S(T)\right]}\right]}\left(\frac{T}{T_0}\right)^3\right\}, \quad (7)$$

where N_{c0}, N_{V0} are the effective density of states in conduction and valence band at T_0 = 300 K, D is the diffusion coefficient.

Temperature dependence of output PV parameters of HJT SCs. In order to investigate the effects of temperature on the output PV parameters of HJT SCs fabricated on *p*-type c-Si substrates, light *J-V* curves were measured under AM0 spectrum (136.7 mW/cm^2) in the temperature range between 173 and 373 K (see Fig. 2). It can be seen in Fig. 2 that ambient temperature has a pronounced impact on the shape of the light *J-V* curves. Specially, the J_{sc} value increases slightly with temperature, while the V_{oc} exhibits a decreasing trend.

As Fig. 2 suggests at elevated temperatures, the influence of series resistance R_s on the shape of the light *J-V* curves becomes less significant, as observed a sharp increase in J_{sc} within this temperature range. In contrast, in the high temperature range, a significant decrease in the shunt resistance R_{sh} is observed, as clearly illustrated by Fig. 2.

In order to investigate the temperature dependence of each output PV parameter, such as V_{oc}, J_{sc}, FF, $P_{\max}$ and η, of HJT SCs fabricated on *p*-type c-Si substrates, we analyzed the variation of all key output characteristics as a function of temperature.

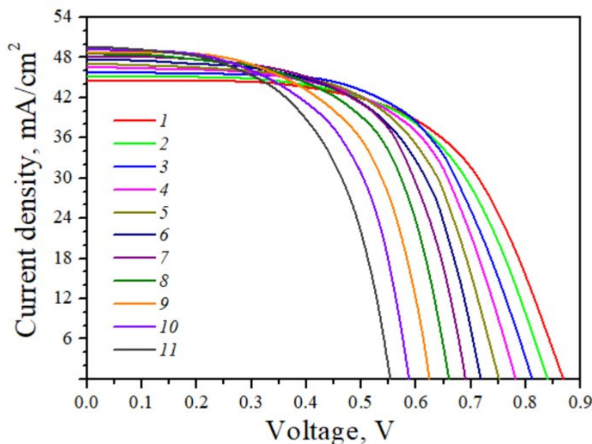

Fig. 2. Light *J-V* curves of HJT SCs based on *p*-type c-Si substrate under AM0 spectrum (136.7 mW/cm^2) in the temperature range between 173 and 373 K.
T, K: 173 (*1*), 193 (*2*), 213 (*3*), 233 (*4*), 253 (*5*), 273 (*6*), 293 (*7*), 313 (*8*), 333 (*9*), 353 (*10*), 373 (*11*)

Fig. 3, *a* presents the temperature dependence of short-circuit current density $J_{sc}(T)$ of HJT SCs based on *p*-type c-Si substrates under AM0 spectrum (136.7 mW/cm^2). The experimental results demonstrate a linear increase in J_{sc} with temperature. For example, the J_{sc} value increased at a rate of 0.028 mA/K from 44.6 mA/cm^2 to ~ 50 mA/cm^2 in the taken temperature range. It is well known that the bandgap of c-Si narrows with increasing temperature [18], causing a shift in the absorption coefficient in the direction of the long-wave region. As a result, the substrate absorbs a broader spectrum of infrared radiation, enhancing electron-hole pair generation in the photoactive region [19, 20].

Based on the experimental results, the temperature coefficients of the short-circuit current density (TCJ_{sc}) was extracted from the slope of the straight-line portion of J_{sc} versus temperature characteristics for HJT SCs based on *p*-type c-Si substrates. The TCJ_{sc} value was

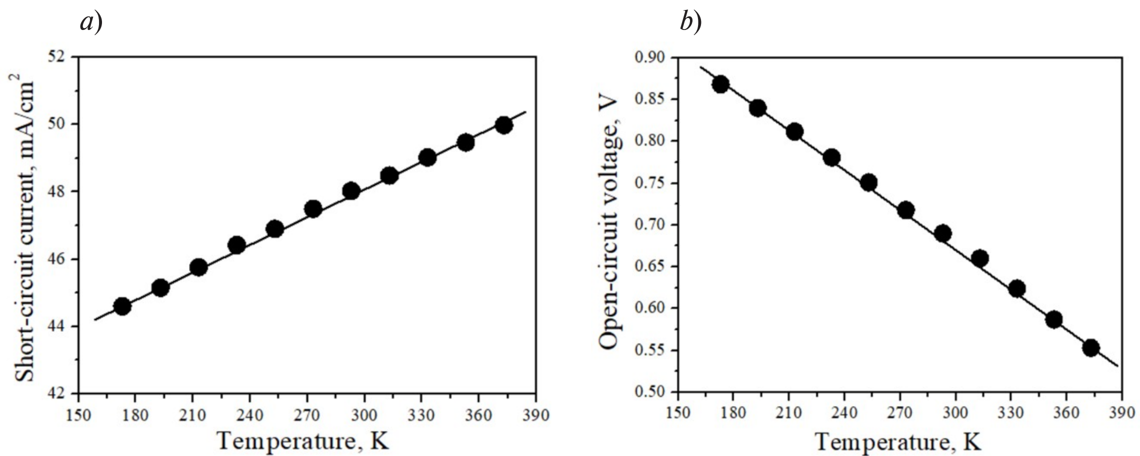

Fig. 3. Temperature dependences of short-circuit current density (*a*) and open-circuit voltage (*b*) of HJT SCs based on *p*-type c-Si substrates under AM0 spectrum

calculated to be 0.058%/K. This value is in good agreement with the previously reported data in Ref. [19].

The experimental results on the temperature dependence of open-circuit voltage $V_{oc}(T)$ for HJT SCs based on *p*-type c-Si substrates under AM0 spectrum (136.7 mW/cm^2) are given in Fig. 3, *b*. As shown, the V_{oc} value decreases linearly with increasing temperature. When decreasing, the V_{qc} takes on values from 0.8684 to 0.5530 V as the temperature increases from 173 to 373 K. This decrease in V_{oc} observed is primarily attributed to the temperature-induced narrowing of the Si bandgap [18], the exponential rise in the reverse saturation current, and the increase in the intrinsic carrier concentration n_i [21], as described by Eq. (5). Simultaneously, according to Eq. (7), PV parameters of HJT SCs, such as J_{sc}, surface $S(T)$ and bulk $\tau(T)$ recombination velocity, acceptor concentration $N_a(T)$ and minority carriers diffusion length L_{diff} exhibit an increasing trend with temperature. Within the temperature range under study, the total surface recombination velocity $S(T)$ in *p*-type HJT SCs increased from 10.6 cm/s at 173 K to 21.8 cm/s at 373 K, which is in good agreement with the data reported in Ref. [22]. The total recombination velocity, encompassing both surface ($S = S_0 + S_d$) and bulk $\tau(T)$ contributions at various temperatures, was estimated using the approach proposed in Refs. [15, 16]. The combined temperature-dependent changes in these parameters contribute to the observed reduction in V_{oc}.

The temperature coefficients of the open-circuit voltage (TCV_{oc}) for HJT SCs based on *p*-type c-Si substrates were determined from the slopes of the straight-line portions of the experimental temperature-dependent curves $V_{oc}(T)$ which exhibited the TCV_{oc} value −0.182% /K in the range from 173 to 373 K. Notably, the obtained value is significantly lower than those reported for other c-Si SCs technologies [7, 19].

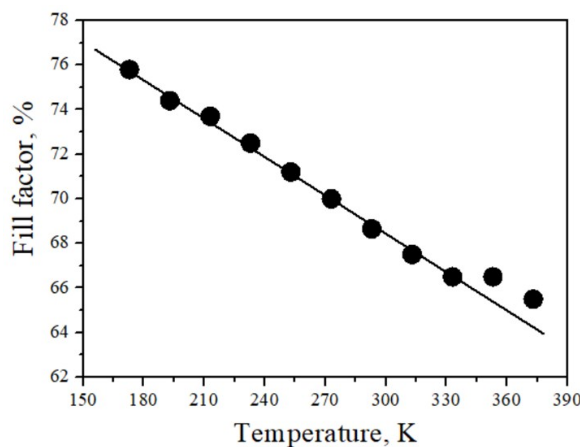

Fig. 4. Temperature dependence of the fill factor of HJT SCs based on *p*-type c-Si substrates under AM0 spectrum

Fig. 4 presents experimental results on the temperature dependence of the fill factor $FF(T)$ of HJT SCs based on *p*-type c-Si substrates under AM0 spectrum (136.7 mW/cm^2). It is well known that the FF is one of the key performance indicators of SCs, reflecting the quality and ideality of the *p*–*n* junction. It is defined by the following expression [20]:

$$FF = \frac{J_m V_m}{J_{sc} V_{oc}}, \quad (8)$$

where J_m, V_m are the current density and the voltage at the maximum power point.

As illustrated in Fig. 4, the FF of the HJT SCs fabricated on *p*-type c-Si exhibits an almost linear decline from 76.0% to approximately

65.5% as the temperature increases from 173 to 373 K. Within this temperature range, the series resistance (R_s) decreases slightly from ~4.9 Ω·cm² to ~2.0 Ω·cm² (see Fig. 5, *a*). In contrast, the shunt resistance (R_{sh}) exhibits a more pronounced linear decrease from ~905 Ω·cm² to ~227 Ω·cm² (Fig. 5, *b*), which significantly contributes to the reduction in the *FF* at elevated temperatures.

In HJT SCs, the R_s was determined from the slope of the *J-V* curve at the open-circuit voltage point, while the R_{sh} was derived from the slope at the short-circuit current point [23].

The R_s of a SC comprises multiple resistive components connected in series with the *p–n* junction, including the bulk resistances of the *p*-type and *n*-type semiconductor regions, the metal-semiconductor contact resistances. Conversely, the R_{sh} characterizes current leakage pathways through, surface recombination currents, bulk defect-assisted tunneling and peripheral leakage at device edges [24].

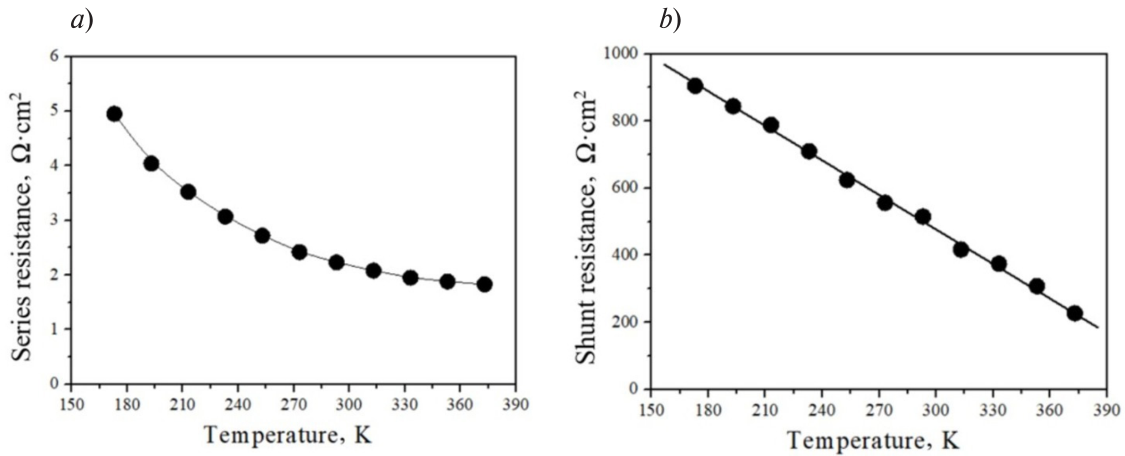

Fig. 5. Temperature dependence of the series (*a*) and shunt resistances (*b*) of HJT SCs based on *p*-type c-Si substrates under AM0 spectrum

It is well known that the *FF* of a SCs is influenced by both R_s and R_{sh}. To achieve a high *FF* value, the series resistance R_s must be minimized, while the shunt resistance R_{sh} should be maximized. In our study, a reduction in the R_s with increasing temperature was clearly observed, which, under typical conditions, should lead to an increase in *FF*. However, the experimental results revealed a contrary behavior, wherein the *FF* decreased with temperature. One of the primary reasons for this discrepancy is the simultaneous reduction in the R_{sh} value due to parasitic leakage paths through *p–n* junction at elevated temperatures (Fig. 5, *b*), as well as the linear decrease in the V_{oc} with temperature. According to Eq. (8), the *FF* exhibits a positive correlation with the V_{oc}, hence, a reduction in the V_{oc} leads to a corresponding decline in the *FF*. As a result, the combined effect of decreasing the R_{sh} and V_{oc} leads to a deterioration of the *FF* with increasing temperature, as confirmed by our experimental data [25].

The temperature coefficient of the *FF* (TC*FF*) and R_{sh} (TCR_{sh}), determined from the slope of the linear decreases in the *FF* and R_{sh}, were found to be −0.077%/K and −0.375%/K, respectively, over the temperature range under study.

Fig. 6 shows the temperature dependence of the maximum output power $P_{max}(T)$ (*a*) and the conversion efficiency $\eta(T)$ (*b*) of the HJT SCs based on *p*-type c-Si substrates under 136.7 mW/cm². The P_{max} value is determined by the product of the J_{sc}, V_{oc} and *FF* values.

As illustrated in Fig. 6, *a*, the P_{max} value of HJT SCs decreases linearly from ~29.5 to ~18.0 mW/cm² with increasing temperature from 273 to 373 K. This behavior of the P_{max} is primarily associated with the temperature dependencies of the key PV parameters such as V_{oc}, *FF*, R_{sh} and R_s, which collectively have the most significant impact on the $P_{max}(T)$ characteristics [26].

The temperature coefficient of the P_{max}(TCP_{max}) for HJT SCs was evaluated to be −0.2% / K in the investigated temperature range. These results demonstrate that the studied *p*-type c-Si HJT SCs exhibit the modest temperature coefficient of the P_{max} among various Si-based PV technologies [7, 19]. The relatively low temperature coefficient of the P_{max} in HJT SCs, compared to those of other Si-based PV technologies, can be attributed to the presence of *i*-α-Si:H passivation layers on both surfaces of the c-Si substrate.

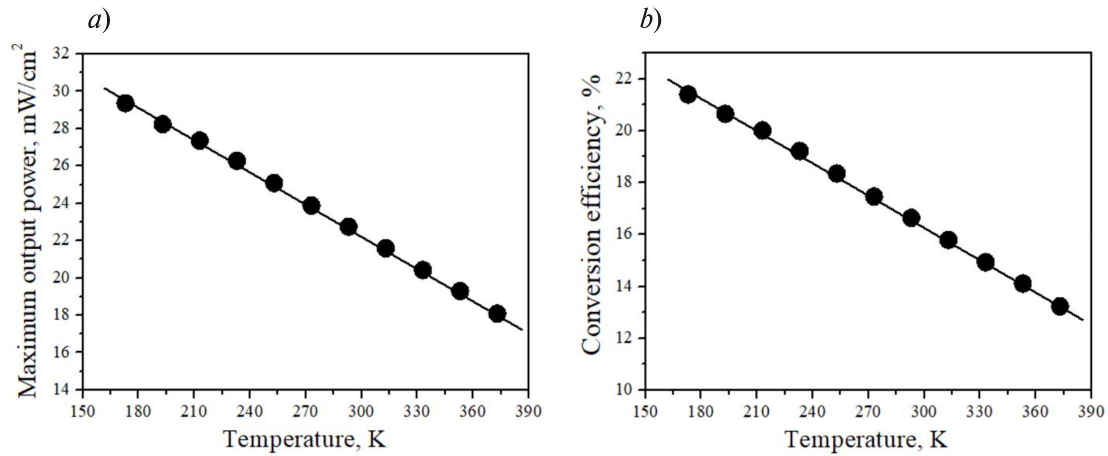

Fig. 6. Temperature dependences of the maximum output power (*a*) and conversion efficiency (*b*) of HJT SCs based on *p*-type c-Si substrates under AM0 spectrum

Fig. 6, *b* shows the experimental results of the temperature dependence of the conversion efficiency $\eta(T)$ of the HJT SCs based on *p*-type c-Si substrates under AM0 (136.7 mW/cm²). The η of the HJT SCs is defined as the ratio of the P_{max} to the incident light power (P_{rad}), which is expressed by the following equation [20]:

$$\eta = \frac{P_{max}}{P_{rad}} \cdot 100\% = \frac{J_{sc} V_{oc} FF}{P_{rad}} \cdot 100\%, \quad (9)$$

where P_{rad} = 136.7 mW/cm².

Referring to Fig. 6, *b*, the η of the HJT SCs based on *p*-type c-Si exhibits a temperature dependence similar to that of the P_{max}. The η values of HJT SCs decrease linearly from ~21.5% at 173 K to ~13.3% at 373 K. According to Ref. [27], the η of HJT SCs can be calculated using the following expression:

$$\eta_c = \eta_{ref} \left[1 - \beta_0 (T_c - T_{ref}) \right], \quad (10)$$

where T_c, T_{ref} are the temperatures of the HJT SCs and the reference (room) temperature (T_{ref} = 298 K), respectively; η_c, η_{ref} are the conversion efficiencies of the HJT SCs at T_c and T_{ref}; β_0 is the temperature coefficient of η ($\eta = -0.002$ K^{-1} for *p*-type c-Si HJT SCs).

As the HJT SC temperature increases, the difference $T_c - T_{ref}$ grows resulting in a linear decrease in the η.

Summary

In this study, the effect of temperature on the *J-V* curves of HJT SCs based on *p*-type c-Si substrates were investigated under AM0 spectrum (136.7 mW/cm²) in the temperature range from 173 to 373 K. The experimental light *J-V* curves of the HJT SCs exhibit an increase in a short-circuit current density with temperature, whereas the open-circuit voltage decreases linearly. Furthermore, the fill factor and shunt resistance degraded significantly with rising temperature, whereas the series resistance showed a moderate reduction. As a result, the maximum output power declined linearly with temperature, with respective temperature coefficient of −0.2% / K. Despite this decline, the studied HJT SCs achieved superior specific power at room temperature.

These findings confirm that gallium-doped *p*-type c-Si-based HJT SCs possess a unique combination of high specific power, low temperature sensitivity, and excellent low-temperature performance. Such characteristics make HJT SCs particularly promising for power generation in small spacecraft (CubeSats) operating in the low-Earth orbit environments.

In future studies, we plan to present experimental results that evaluate the combined impact of radiation and temperature on the photovoltaic (PV) performance of the HJT SCs.

REFERENCES

1. **Hassan Q., Viktor P., Al-Musawi T.J., et al.,** The renewable energy role in the global energy transformations, Renew. Energy Focus. 48 (2024) 100545.

2. **Machin A., Marquez F.,** Advancements in photovoltaic cell materials: Silicon, organic and perovskite solar cells, Materials. 17 (5) (2024) 1165.

3. **Green M. A., Dunlop E. D., Yoshita M., et al.,** Solar cell efficiency tables (Version 64), Prog. Photovolt.: Res. Appl. 32 (7) (2024) 425–441.

4. **Lv X., Hu Z., Yang J., et al.,** Transmission electron microscopy study on the laser-cutting induced microdefects in silicon heterojunction solar cells, Sol. Energy Mater. Sol. Cells. 292 (15 Oct) (2025) 113792.

5. **Lin H., Yang M., Ru X., et al.,** Silicon heterojunction solar cells with up to 26.81% efficiency achieved by electrically optimized nanocrystalline silicon hole contact layers, Nat. Energy. 8 (8) (2023) 789–799.

6. **Joseph K. L. V., Rosana N. T. M., Kumar J. A., Samrot A. V.,** Commercial bifacial silicon solar cells – characteristics, module topology and passivation technique for high electrical output: An overview, Results Eng. 26 (June) (2025) 104971.

7. **Le A. H. T., Basnet R., Yan D., et al.,** Temperature-dependence performance of silicon solar cells with polysilicon passivating contacts, Sol. Energy Mater. Sol. Cells. 225 (15 June) (2021) 111020.

8. **Singh P., Singh S. N., Lal M., Husain M.,** Temperature dependence of I-V characteristics and performance parameters of silicon solar cell, Sol. Energy Mater. Sol. Cells. 92 (Dec) (2008) 1611–1616.

9. **Thirsk R., Kuipers A., Mukai C., Williams D.,** The space-flight environment: The international Space Station and beyond, Can. Med. Assoc. J. 180 (12) (2009) 1216–1220.

10. **Buitrago-Leiva J. N., El Khayati Ramouz M., Camps A., Ruiz-de-Azua J. A.,** Statistical analysis of LEO and GEO satellite anomalies and space radiation, Aerosp. 11 (11) (2024) 924.

11. **Ataboev O. K., Terukov E. I., Shelopin G. G., Kabulov R. R.,** Wet chemical treatment of monocrystalline silicon wafer surfaces, Appl. Sol. Energy. 57 (5) (2021) 363–369.

12. **Wolf S. D., Olibet S., Ballif C.,** Stretched-exponential α-Si:H/c-Si interface recombination decay, Appl. Phys. Lett. 93 (9) (2008) 032101.

13. **Kumar R., Jain P. K.,** Impact of temperature on the performance of efficient GaInP single-junction solar cells with double back surface field, MRS Adv. 10 (12) (2025) 1536–1544.

14. **Acharyya S., Ghosh D. K., Banerjee D., Maity S.,** Analyzing the operational versatility of advanced IBC solar cells at different temperatures and also with variation in minority carrier lifetimes, J. Comput. Electron. 23 (6) (2024) 1170–1194.

15. **Panaiotti I. E., Terukov E. I.,** A study of the effect of radiation on recombination loss in heterojunction solar cells based on single-crystal silicon, Tech. Phys. Lett. 45 (3) (2019) 193–196.

16. **Panaiotti I. E., Terukov E. I., Shakhrai I. S.,** A method for calculating operating characteristics of silicon heterojunction solar cells with arbitrary parameters of crystalline substrates, Tech. Phys. Lett. 46 (9) (2020) 835–837.

17. **Ataboev O. K., Utamuradova Sh. B., Panaiotti I. E., et al.,** Temperature dependence of photovoltaic performance of silicon heterojunction solar cells based on gallium- and phosphorous-doped silicon wafers, Radiat. Phys. Chem. 240 (March) (2026) 113407.

18. **Bludau W., Onton A., Heinke W.,** Temperature dependence of the band gap of silicon, J. Appl. Phys. 45 (4) (1974) 1846–1848.

19. **Haschke J., Seif J. P., Riesen Y., et al.,** The impact of silicon solar cell architecture and cell interconnection on energy yield in hot and sunny climates, Energy Environ. Sci. 10 (5) (2017) 1–11.

20. **Ataboev O. K., Kabulov R. R., Matchanov N. A., Egamov S. R.,** Influence of temperature on the output parameters of a photovoltaic module based on amorphous hydrogenated silicon, Appl. Sol. Energy. 55 (3) (2019) 159–167.

21. **Löper P., Pysch D., Richter A., et al.,** Analysis of the temperature dependence of the open-circuit voltage, Energy Procedia. 27 (2012) 135–142.

22. **Bernardini S., Bertoni M. I.,** Insights into the degradation of amorphous silicon passivation layer for heterojunction solar cells, Phys. Status Solidi A. 216 (4) (2019) 1800705.

23. **Singh P., Ravindra N. M.,** Analysis of series and shunt resistance in silicon solar cells using single and double exponential models, Emerg. Mater. Res. 1 (1) (2011) 33–38.

24. **Fahrenbruch A. L., Bube R. H.,** Fundamentals of solar cells. Photovoltaic solar energy conversion, Academic Press, New York, 1983. 559 p.

25. **Büyükbaş-Uluşan A., Turan R., Altındal Ş.,** On the investigation of current transport mechanisms (CTMs) of the crystalline Si solar cells utilizing current/voltage (I-V) characteristics in temperature range of 110–380 K, J. Mater. Sci. Mater. Electron. 36 (19) (2025) 1173.

26. **Green M. A.,** General temperature dependence of solar cell performance and implications for device modelling, Progr. Photovol. Res. Appl. 11 (5) (2003) 333–340.

27. **Dubey S., Sarvaiya J. N., Seshadri B.,** Temperature dependent photovoltaic efficiency and its effect on PV production in the world – A review, Energy Procedia. 33 (2013) 311–321.

СПИСОК ЛИТЕРАТУРЫ

1. **Hassan Q., Viktor P., Al-Musawi T. J., Ali B. M., Algburi S., Alzoubi H. M., Al-Jiboory A. K., Sameen A. Z., Salman H. M., Jaszczur M.** The renewable energy role in the global energy transformations // Renewable Energy Focus. 2024. Vol. 48. March. P. 100545.

2. **Machin A., Marquez F.** Advancements in photovoltaic cell materials: Silicon, organic and perovskite solar cells // Materials. 2024. Vol. 17. No. 5. P. 1165.

3. **Green M. A., Dunlop E. D., Yoshita M., Kopidakis N., Bothe K., Siefer G., Hinken D., Rauer M., Hohl-Ebinger J., Hao X.** Solar cell efficiency tables (Version 64) // Progress in Photovoltaics: Research and Applications. 2024. Vol. 32. No. 7. Pp. 425–441.

4. **Lv X., Hu Z., Yang J., Yu X., Jin C., Yang D.** Transmission electron microscopy study on the laser-cutting induced microdefects in silicon heterojunction solar cells // Solar Energy Materials and Solar Cells. 2025. Vol. 292. 15 October. P. 113792.

5. **Lin H., Yang M., Ru X., et al.** Silicon heterojunction solar cells with up to 26.81% efficiency achieved by electrically optimized nanocrystalline silicon hole contact layers // Nature Energy. 2023. Vol. 8. No. 8. Pp. 789–799.

6. **Joseph K. L. V., Rosana N. T. M., Kumar J. A., Samrot A. V.** Commercial bifacial silicon solar cells – characteristics, module topology and passivation technique for high electrical output: An overview // Results in Engineering. 2025. Vol. 26. June. P. 104971.

7. **Le A. H. T., Basnet R., Yan D., Chen W., Nandakumar N., Duttagupta S., Seif J. P., Hameiri Z.** Temperature-dependence performance of silicon solar cells with polysilicon passivating contacts // Solar Energy Materials and Solar Cells. 2021. Vol. 225. 15 June. P. 111020.

8. **Singh P., Singh S. N., Lal M., Husain M.** Temperature dependence of I-V characteristics and performance parameters of silicon solar cell // Solar Energy Materials and Solar Cells. 2008. Vol. 92. December. Pp. 1611–1616.

9. **Thirsk R., Kuipers A., Mukai C., Williams D.** The space-flight environment: The international Space Station and beyond // Canadian Medical Association Journal. 2009. Vol. 180. No. 12. Pp. 1216–1220.

10. **Buitrago-Leiva J. N., El Khayati Ramouz M., Camps A., Ruiz-de-Azua J. A.** Statistical analysis of LEO and GEO satellite anomalies and space radiation // Aerospace.2024. Vol. 11. No. 11. P. 924.

11. **Ataboev O. K., Terukov E. I., Shelopin G. G., Kabulov R. R.** Wet chemical treatment of monocrystalline silicon wafer surfaces // Applied Solar Energy. 2021. Vol. 57. No. 5. Pp. 363–369.

12. **Wolf S. D., Olibet S., Ballif C.** Stretched-exponential α-Si:H/c-Si interface recombination decay // Applied Physics Letters. 2008. Vol. 93. No. 9. P. 032101.

13. **Kumar R., Jain P. K.** Impact of temperature on the performance of efficient GaInP single-junction solar cells with double back surface field // MRS Advances. 2025. Vol. 10. No. 12. Pp. 1536–1544.

14. **Acharyya S., Ghosh D. K., Banerjee D., Maity S.** Analyzing the operational versatility of advanced IBC solar cells at different temperatures and also with variation in minority carrier lifetimes // Journal of Computational Electronics. 2024. Vol. 23. No. 6. Pp. 1170–1194.

15. **Панайотти И. Е., Теруков Е. И.** Исследование влияния радиации на рекомбинационные потери в гетеропереходных солнечных элементах на основе поликристаллического кремния // Письма в Журнал технической физики. 2019. Т. 45. № 5. С. 9–12.

16. **Панайотти И. Е., Теруков Е. И., Шахрай И. С.** Метод расчета рабочих характеристик кремниевых гетеропереходных солнечных элементов с произвольными параметрами кристаллической подложки // Письма в Журнал технической физики. 2020. Т. 46. № 17 (173). С. 3–5.

17. **Ataboev O. K., Utamuradova Sh. B., Panaiotti I. E., Terukov E. I., Malevskiy D. A., Baranov A. I., Troshin A. V.** Temperature dependence of photovoltaic performance of silicon heterojunction solar cells based on gallium- and phosphorous-doped silicon wafers // Radiation Physics and Chemistry. 2026. Vol. 240. March. P. 113407.

18. **Bludau W., Onton A., Heinke W.** Temperature dependence of the band gap of silicon // Journal of Applied Physics. 1974. Vol. 45. No. 4. Pp. 1846–1848.

19. **Haschke J., Seif J. P., Riesen Y., et al.** The impact of silicon solar cell architecture and cell interconnection on energy yield in hot and sunny climates // Energy and Environmental Science. 2017. Vol. 10. No. 5. Pp. 1–11.

20. **Ataboev O. K., Kabulov R. R., Matchanov N. A., Egamov S. R.** Influence of temperature on the output parameters of a photovoltaic module based on amorphous hydrogenated silicon // Applied Solar Energy. 2019. Vol. 55. No. 3. Pp. 159–167.

21. **Löper P., Pysch D., Richter A., Hermle M., Janz S., Zacharias M., Glunz S. W.** Analysis of the temperature dependence of the open-circuit voltage // Energy Procedia. 2012. Vol. 27. Pp. 135–142.

22. **Bernardini S., Bertoni M. I.** Insights into the degradation of amorphous silicon passivation layer for heterojunction solar cells // Physica Status Solidi A. 2019. Vol. 216. No. 4. P. 1800705.

23. **Singh P., Ravindra N. M.** Analysis of series and shunt resistance in silicon solar cells using single and double exponential models // Emerging Materials Research. 2011. Vol. 1. No. 1. Pp. 33–38.

24. **Фаренбрух А., Бьюб Р.** Солнечные элементы: Теория и эксперимент. Пер. с англ. М.: Энергоатомиздат, 1987. 280 с.

25. **Büyükbaş-Uluşan A., Turan R., Altındal Ş**. On the investigation of current transport mechanisms (CTMs) of the crystalline Si solar cells utilizing current/voltage (I-V) characteristics in temperature range of 110–380 K // Journal of Materials Science: Materials in Electronics. 2025. Vol. 36. No. 19. P. 1173.

26. **Green M. A.** General temperature dependence of solar cell performance and implications for device modelling // Progress in Photovoltaics: Research and Applications. 2003. Vol. 11. No. 5. Pp. 333–340.

27. **Dubey S., Sarvaiya J. N., Seshadri B.** Temperature dependent photovoltaic efficiency and its effect on PV production in the world – A review // Energy Procedia. 2013. Vol. 33. Pp. 311–321.

THE AUTHORS

ATABOEV Omonboy K.

Research Institute of Semiconductor Physics and Microelectronics at the National University of Uzbekistan named after Mirzo Ulugbek.

20, Yangi Olmazor St., Tashkent, 100057, Republic of Uzbekistan

omonboy12@mail.ru

ORCID: 0000-0002-5226-1101

UTAMURADOVA Sharifa B.

Research Institute of Semiconductor Physics and Microelectronics at the National University of Uzbekistan named after Mirzo Ulugbek.

20, Yangi Olmazor St., Tashkent, 100057, Republic of Uzbekistan

sh-utamuradova@yandex.com

ORCID: 0000-0002-1718-1122

TERUKOV Evgeniy I.

Ioffe Institute, RAS

26, Polytekhnicheskaya St., St. Petersburg, 194021, Russia

e.terukov@hevelsolar.com

ORCID: 0000-0002-5226-1101

BARANOV Artem I.
Alferov University, RAS
8-3 Khlopin St., St. Petersburg, 194021, Russia
Itiomchik@yandex.ru
ORCID: 0000-0002-5226-1101

INIYATOVA Klara Kh.
Nukus State Technical University
74, A. Dosnazarov St., Nukus, Karakalpakstan, 230100, Republic of Uzbekistan
klarainiyatova2002@gmail.com

СВЕДЕНИЯ ОБ АВТОРАХ

АТАБОЕВ Омонбой Курбанбоевич – *кандидат физико-математических наук, старший научный сотрудник Научно-исследовательского института физики полупроводников и микроэлектроники при Национальном университете Узбекистана имени Мирзо Улугбека, г. Ташкент, Республика Узбекистан.*
100057, Республика Узбекистан, г. Ташкент, ул. Янги Олмазор, 20.
omonboy12@mail.ru
ORCID: 0000-0002-5226-1101

УТАМУРАДОВА Шарифа Бекмурадовна – *доктор физико-математических наук, профессор Научно-исследовательского института физики полупроводников и микроэлектроники при Национальном университете Узбекистана имени Мирзо Улугбека, г. Ташкент, Республика Узбекистан.*
100057, Республика Узбекистан, г. Ташкент, ул. Янги Олмазор, 20.
sh-utamuradova@yandex.com
ORCID: 0000-0002-1718-1122

ТЕРУКОВ Евгений Иванович – *доктор технических наук, профессор Физико-технического института имени А. Ф. Иоффе РАН, Санкт-Петербург, Россия.*
194021, Россия, г. Санкт-Петербург, Политехническая ул., 26
e.terukov@hevelsolar.com
ORCID: 0000-0002-5226-1101

БАРАНОВ Артем Игоревич – *кандидат физико-математических наук, старший научный сотрудник Академического университета имени Ж. И. Алфёрова РАН, Санкт-Петербург, Россия.*
194021, Россия, г. Санкт-Петербург, ул. Хлопина, 8, к. 3
Itiomchik@yandex.ru
ORCID: 0000-0002-5226-1101

ИНИЯТОВА Клара Хамидуллаевна – *M. Sc., старший преподаватель Нукусского государственного технического университета, г. Нукус, Каракалпакстан, Республика Узбекистан.*
230100, Республика Узбекистан, Каракалпакстан, г. Нукус, ул. А. Досназарова, 74
klarainiyatova2002@gmail.com

Received 17.08.2025. Approved after reviewing 05.09.2025. Accepted 19.01.2026.
Статья поступила в редакцию 17.08.2025. Одобрена после рецензирования 05.09.2025. Принята 19.01.2026.

© Санкт-Петербургский политехнический университет Петра Великого, 2026